

Phase Slips and Interfaces in D -Wave Superconductors.

Andrew M. Martin[†] and James F. Annett[§]

[†]*Département de Physique Théorique, Université de Genève 4, Switzerland.*

[§]*University of Bristol, H.H. Wills Physics Laboratory, Royal Fort, Tyndall Ave, Bristol BS8 1TL, United Kingdom.*
(April 26, 2024)

We consider a model (100) interface between two d -wave superconductors. By solving the Bogoliubov de Gennes equation on a tight binding lattice, we study the properties of the interface as a function of the interface barrier. We contrast the two scenarios: (i) an order parameter phase difference of $\theta = 0$ across the interface, and (ii) a phase slip of $\theta = \pi$ across the interface. We find resonant sub-gap structure in the density of states only when there is a phase slip present. We show that the local s -wave and “ p -wave like” order parameter components are strongly influenced by the barrier profile and by the phase slip. The temperature dependence of the local p -wave order parameter follows the underlying bulk T_c for p -wave superconductivity implying that this could be measured by a suitable tunneling experiment. We also calculate the Josephson critical current as a function of the strength of the insulating barrier at the interface.

Pacs numbers: 74.50.+r, 74.60.Jg, 74.80.-g

I. INTRODUCTION.

Over the past few years it has been generally agreed that the macroscopic symmetry of the superconducting order parameter in high T_c superconductors is unconventional. The pairing state is almost certainly d -wave [1–3], either pure $d_{x^2-y^2}$ or a mixed state such as $d + s$ [4] or $d + is$ [5], which is predominantly d -wave. The d -wave pairing state raises many important questions, such as the relationship between the pairing state and the physical properties of the superconductors, and of course, the microscopic origin of the pairing interaction itself.

In particular it becomes interesting to consider the microscopic properties of the interfaces of d -wave symmetry systems. This is necessary both to understand the physical properties of high T_c materials, and to develop further tests of the pairing state and order parameter. For example, it has already been shown that at a normal metal to d -wave superconductor ($N - D$) interface there is an extended s -wave component to the order parameter in the region of the interface and that this survives up to a few coherence lengths away from the interface [6–9]. There is also experimental and theoretical evidence for microscopic time reversal symmetry breaking at such interfaces [10,11]. The presence or absence of such subdominant order parameters can, in principle, be used to extract information about the nature of the microscopic pairing interaction. For example some models will allow both d and s -wave pairing, while other models are pair breaking in the s -wave channel. There has also been a substantial amount of work concerning the effect of d -wave symmetry on the Josephson Effect [12–16], mesoscopic scattering properties of $N - I - D$ structures [17–20] and tunneling density of states for surfaces of d -wave superconductors [21,22].

In this paper we examine the self-consistent changes in

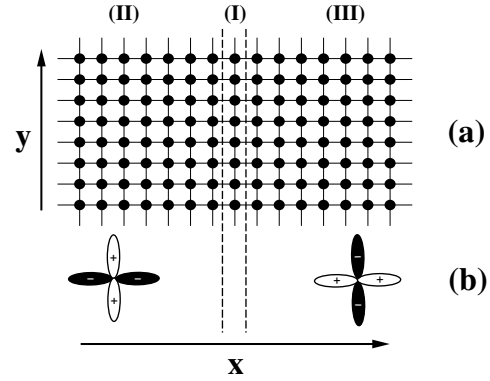


FIG. 1. A schematic diagram of the system we wish to consider. Regions I, II and III represent a tight binding lattice, where regions II and III are connected to each other via an interface (region I). In regions II and III we can define the symmetry of the superconducting order parameter to be mismatched by π .

the superconducting order parameter near an insulating barrier between two d -wave superconductors, i.e. a $D - I - D$ interface. The basic geometry is shown in Fig. 1. We carry out a detailed study of how the interface properties evolve as the strength of the barrier is increased from a small perturbation to a strong tunneling barrier. In this way we can contrast the behaviour of interfaces with little or no tunnel barrier, such as twin boundaries, to interfaces with a strong tunnel barrier, such as tunneling through vacuum or oxygen depleted regions at the surface. Our results may also be relevant as a model of grain boundary junctions in high T_c materials, since Gurevich and Pashitskii have proposed that these junctions are essentially $D - I - D$ junctions whose impurity barrier is simply dependent up the angle of the grain boundary [23].

In our calculations we will concern ourselves with two

scenarios (i) where there is no phase difference in the order parameter over the interface ($\theta = 0$) and (ii) where there is an imposed phase slip of π over the interface ($\theta = \pi$), as illustrated in Fig. 1. For both of these scenarios we focus our attention on the magnitude of the extended s -wave and “ p -wave like” components of the order parameter in the region of the interface. There is already a great interest in the role extended s -wave components have to play in the region of twin-boundaries, for example W. Belzig, C. Bruder and M. Sigrist [11] have studied how the local density of states is modified, as one moves across a twin boundary when the bulk order parameter is $d \pm i s$ and the effect of temperature on these calculations.

The plan of this paper is as follows. In Sec. II we describe briefly the model Hamiltonian, and the methodology used to solve the Bogoliubov de Gennes equation in our system. Then in Sec. III we will describe, in detail, the system of interest and define the different components of the superconducting order parameter which will be relevant. In Sec. IV we present results for a perfect interface, i.e. the limit that the tunnel barrier height is zero. We note that in this *clean* case an order parameter phase change of $\theta = \pi$ across the “interface” corresponds to a phase slip of π in a perfect superconductor. We establish that this phase slip is a stable soliton like solution of the Bogoliubov de Gennes equation and we obtain the local density of electronic states in the vicinity of the phase slip. We then proceed to analyze the different components to the superconducting order parameter at the centre of the phase slip and how these change as we change the temperature of the system. In Sec V we turn our attention to $D - I - D$ interfaces, calculating the properties of the interface as a function of the tunnel barrier height for both the scenarios $\theta = 0$ and $\theta = \pi$. Finally we conclude with comparisons of the local particle density of states in the region of the interface. Using these local particle density of states we also estimate how the Josephson critical current is changed as the tunnel barrier strength is changed.

II. THE BOGOLIUBOV DE GENNES EQUATION.

Our starting point is the Bogoliubov de Gennes (BdG) equation,

$$\sum_j \mathbf{H}_{ij} \begin{pmatrix} u_j^n \\ v_j^n \end{pmatrix} = E_n \begin{pmatrix} u_i^n \\ v_i^n \end{pmatrix} \quad (1)$$

where u_i^n and v_i^n are the particle and hole amplitudes on site i associated with eigenenergy E_n . The Hamiltonian is

$$\mathbf{H}_{ij} = \begin{pmatrix} H_{ij} & \Delta_{ij} \\ \Delta_{ij}^* & -H_{ij}^* \end{pmatrix}, \quad (2)$$

where H_{ij} is the normal part of the tight binding Hamiltonian and Δ_{ij} is the anomalous part, given by the BCS gap function.

In the case of the cuprates we have $d_{x^2-y^2}$ pairing on a square two-dimensional lattice. The simplest model Hamiltonian which leads to this pairing state is the non-local attractive Hubbard model,

$$\hat{H} = \sum_i \epsilon_i c_{i\sigma}^\dagger c_{i\sigma} + \sum_{\langle ij \rangle} \left(t_{ij} (c_{i\sigma}^\dagger c_{j\sigma} + \text{h.c.}) - \frac{U_{ij}}{2} \hat{n}_i \hat{n}_j \right), \quad (3)$$

where, as usual, $c_{i\sigma}^\dagger$ and $c_{i\sigma}$ are the electron creation and annihilation operators at site i for spin σ and \hat{n}_i is the number operator at site i . For simplicity we shall assume that both t_{ij} and U_{ij} are limited to nearest neighbors only. We shall neglect any on-site interactions U_{ii} . Also, for simplicity, we neglect retardation in the attractive interaction.

The BdG equation, Eq. 1 is easily derived as the appropriate mean field factorization of the Hubbard model Eq. 3. The normal part of the Hamiltonian Eq. 2, H_{ij} , is given by

$$H_{ij} = (\epsilon'_i - \mu) \delta_{ij} + t'_{ij} (1 - \delta_{ij}) \quad (4)$$

where μ is the chemical potential. The on-site energy, ϵ'_i , includes the bare on-site energy and the normal Hartree potential

$$\epsilon'_i = \epsilon_i + \sum_j U_{ij} n_{jj} \quad (5)$$

where n_{jj} is the charge density at site j . Similarly the self-consistent hopping t'_{ij} is the bare hopping plus a Hartree-Fock exchange term

$$t'_{ij} = t_{ij} + \frac{1}{2} U_{ij} n_{ij}. \quad (6)$$

The charge densities n_{ii} and n_{ij} are determined from the eigenvectors of the Hamiltonian Eq. 1 and are given by

$$\begin{aligned} n_{ij} &= \sum_\sigma \langle \Psi_{i\sigma}^\dagger \Psi_{j\sigma} \rangle \\ &= 2 \sum_n [(u_i^n)^* u_j^n f(E_n) + v_i^n (v_j^n)^* (1 - f(E_n))] \end{aligned} \quad (7)$$

where the sum is over all of the *negative* eigenvalues E_n only.

The off-diagonal part of the mean field Hamiltonian Eq. 2 is the pairing potential or gap function, Δ_{ij} . Self-consistently this is determined from

$$\Delta_{ij} = -U_{ij} F_{ij} \quad (8)$$

where the anomalous density is

$$F_{ij} = \langle \Psi_{i\uparrow} \Psi_{j\downarrow} \rangle \\ = \sum_n [u_i^n (v_j^n)^* (1 - f(E_n)) - (v_i^n)^* (u_j^n) f(E_n)] \quad (9)$$

and again the sum only includes eigenvalues E_n up to the condensate chemical potential (μ).

In the case of a bulk square lattice with nearest neighbour attractions U_{ij} and nearest neighbour hopping the solutions to the above set of self-consistent equations are well known. Depending on the band filling and temperature the gap function Δ_{ij} may be pure $d_{x^2-y^2}$, pure extended s -wave or a $d+is$ mixed state [24]. In this paper we shall work exclusively near half filling where only the pure d -wave state is stable.

To solve the above system of self-consistent equations we employ the Recursion Method [9,25,31,27] following exactly the method outlined in [9]. The advantage of this method is that it is a purely real-space calculation, and so it is not necessary to assume periodic boundary conditions. For example, in the interface geometry studied in this paper we have two semi-infinite lattices joined at an interface. The recursion method also gives directly the local density of states, $N(E)$, at any given site, which, as we shall show below, assists in the physical interpretation of the self-consistent numerical results.

III. INTERFACE GEOMETRY.

In the cuprate superconductors there are a number of important intrinsic weak links, including twin boundaries, low angle grain boundaries, and edge dislocations. There are also a number of man made interfaces designed for specific applications, including break junctions, high angle grain boundary junctions, ramp junctions, and junctions with electron and ion beam irradiated barrier regions. In separate papers we have investigated simple $S-N$, $D-N$ and $S-D$ interfaces [9], and examined in detail the behaviour of a $D-D$ high angle grain boundary junction [28]. In this paper we seek to examine how the interface properties are modified by the presence of an insulating barrier. For example the insulating barrier may be caused by oxygen depletion in the region of the interface, as suggested by Gurevich and Pashitskii in their model of grain boundaries [23].

With this motivation, we shall study in detail the system shown in Fig. 1(a). We have two semi-infinite d -wave superconducting regions (II) and (III) which are connected to each other via an interface (I). We study (100) oriented interfaces as shown in Fig. 1(a). In the interface region (I) we define the strength of the barrier, V , by setting $\epsilon'_i = V$ in this region to be finite, compared to the rest of the system where $\epsilon'_i = 0$. This barrier height could physically represent the amount of oxygen depletion at the interface, or the vacuum or insulating barrier width in the case of (100) surface tunnel junctions. We

shall examine the changes in the interface properties as the barrier height V is varied from zero to a large value.

We shall study the Josephson energy of the junction by comparing the cases of either zero or π phase difference between the bulk order parameters far from the interface. Fig. 1(b) illustrates the case of a π phase difference in the d -wave order parameter. We carry out the calculation by imposing a fixed bulk d -wave order parameter Δ_{ij} far from the interface, and then self-consistently computing the Δ_{ij} in the region near to the interface. Typically we perform the self-consistent calculations in a region of width five coherence lengths on either side of the junction, confirming that after this distance the self-consistent parameters have returned to their bulk values.

The self-consistent order parameters Δ_{ij} are computed for each nearest neighbour bond $\langle ij \rangle$ in the lattice ($\Delta_{ij} = \Delta_{ji}$). However interpreting these results is simplified if we decompose these Δ_{ij} into components of different symmetries. For this reason we define the following four linear combinations at each site i ,

$$\begin{aligned} \Delta_i^{(d)} &= \frac{1}{4} \Delta_{ij_1} - \Delta_{ij_2} + \Delta_{ij_3} - \Delta_{ij_4} \\ \Delta_i^{(s)} &= \frac{1}{4} \Delta_{ij_1} + \Delta_{ij_2} + \Delta_{ij_3} + \Delta_{ij_4} \\ \Delta_i^{(p_x)} &= \frac{1}{2} \Delta_{ij_1} - \Delta_{ij_3} \\ \Delta_i^{(p_y)} &= \frac{1}{2} \Delta_{ij_2} - \Delta_{ij_4}. \end{aligned}$$

Here the sites $j_1 \dots j_4$ are the four nearest neighbours of site i , say counting clockwise. The first two combinations are simply $d_{x^2-y^2}$ and extended s -wave pairing respectively. The second two correspond to components of the Δ_{ij} which are *odd* about site i . For this reason they may be said to be “ p -wave like” components of the order parameter. It is important to note that these components do not truly correspond to p -wave pairing since they are spin singlet not triplet and there is no spontaneous breaking of spin rotational symmetry. These two terms are more closely related to *gradients* of s or d -wave order parameters. They also have some relationship to Yang’s η pairing order parameter [29] which is a spin singlet order parameter, but one that alternates sign on neighboring lattice sites. This has also been referred to elsewhere as *antiferrosuperconductivity* [30,31]. Here $\Delta^{(p_x)}$ and $\Delta^{(p_y)}$ correspond to an alternating non-local order parameter Δ_{ij} , unlike η -pairing which corresponds to a staggered Δ_{ii} on-site gap function. Note that because the system in Fig. 1(a) is perfectly periodic in y we shall always have $\Delta_i^{(p_y)} = 0$.

For our chosen model parameters only the d -wave component $\Delta_i^{(d)}$ is non-zero in the bulk far from the interface. However components of the other types can arise near the interface driven by the local symmetry breaking. The self-consistent order parameter can also have

spontaneous symmetry breaking phase transitions as a function of temperature or chemical potential, for example breaking of time reversal symmetry into an $d+is$ type state.

IV. INTERFACE PROPERTIES: NO BARRIER

Having outlined in previous sections the method for calculating and analyzing the properties of the order parameter, we now consider the most simple situation: $V = 0$ throughout the system. In this case there is no barrier at all at the interface I . If the bulk phase difference across the system θ is zero then we obviously have just a simple bulk system everywhere with the bulk d -wave order parameter.

On the other hand if $\theta = \pi$ (Fig. 1(b)) then we have a *phase slip* in the unit cell. This is the superconducting analogue of a Bloch wall separating magnetic domains. By solving the Bogoliubov de Gennes equations self-consistently we can calculate the width of the phase slip region and the variation of the order parameter across the phase slip.

Fig. 2 shows our self-consistently determined order parameters in this phase slip geometry. Since all quantities only vary in the x direction, we can plot $|\Delta^{(d)}(x)|$, $|\Delta^{(s)}(x)|$, $|\Delta^{(p_x)}(x)|$ in the region of the interface ($x = 0$), noting that $|\Delta^{(p_y)}(x)| = 0$. We started the self-consistent calculation by imposing a d -wave order parameter throughout the system, but with a phase change of π at $x = 0$. The solution was then determined self-consistently by iterating the BdG equations starting from this state. We find that the phase slip is a stable self-consistent solution of the BdG equations.

In Fig. 2 we can see how the $|\Delta^{(d)}(x)|$ (solid line) varies in the region of the interface. It is clearly a minimum at the interface and quickly reaches its bulk value, oscillat-

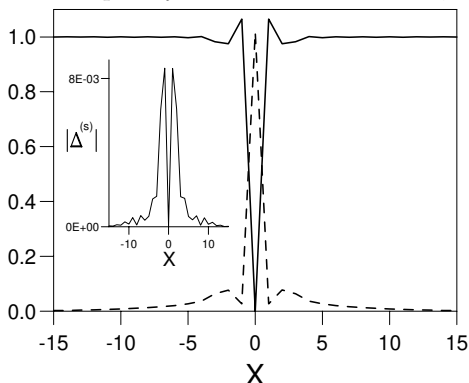


FIG. 2. Profiles of different symmetry components of the superconducting order parameter in the presence of a $\theta = \pi$ phase slip, $|\Delta^{(d)}(x)|/|\Delta^{(d)}(\infty)|$ (solid line) and $|\Delta^{(p_x)}(x)|/|\Delta^{(d)}(\infty)|$ (dashed line). The insert shows $|\Delta^{(s)}(x)|$ in the region of the interface. For all of these figures $T = 0$ and the barrier height is $V = 0$.

ing as it does [32,33]. The extended s -wave component $|\Delta^{(s)}(x)|$ (insert) is also a minimum at the interface, but it then reaches a maximum close to the interface and then reduces to zero in the bulk. On the other hand $|\Delta^{(p_x)}(x)|$ (dashed line) has a strong maximum at the interface.

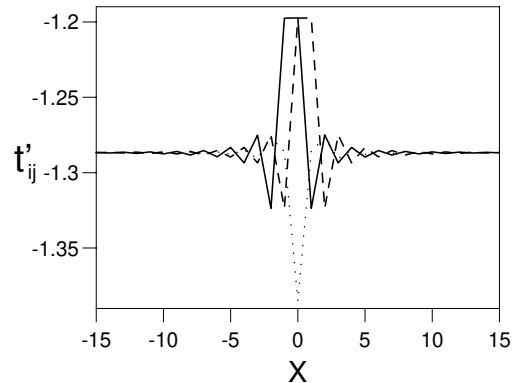


FIG. 3. The effective hopping t'_{ij} as a function of distance from the interface ($x = 0$). The hoppings are $t'_{j1}(x)$ (solid line), $t'_{j2}(x)$ (dotted line), $t'_{j3}(x)$ (dashed line) and $t'_{j4}(x)$ (dotted line), where j_1 to j_4 correspond to the four different nearest neighbour bonds. All parameters are the same as in Fig. 2.

It is also interesting to consider the self-consistent hopping, t'_{ij} , in the region of the barrier. Again, considering that each site i has four neighbours $j_1 \dots j_4$ we can plot the four components $t'_{ij_1} \dots t'_{ij_4}$ as a function of position. Changing notation slightly we can think of these as four functions of position, x , $t'_j(x)$ ($j = 1..4$). In Fig. 3 the dashed and solid lines show $t'_1(x)$ and $t'_3(x)$ respectively (the hopping perpendicular to the interface) and the dotted line is $t'_2(x)$ ($= t'_4(x)$), (the hopping parallel to the interface). The plot shows that in the region of the interface the hopping is modified from its bulk value. It is this modification of the hopping which helps stabilize the phase slip, this is analogous to the case of conventional local s -wave pairing where modification of the local density in the region of the phase slip enhances its stability [34]. The oscillations in the t'_{ij} shown in Fig. 3 simply correspond to Friedel oscillations in the non-local Hartree-Fock exchange term ($\frac{U_{ij}n_{ij}}{2}$). These oscillations are exactly analogous to the Friedel oscillations around an impurity or surface in a normal system, even though there is no *normal* barrier V here.

The results shown in Figs. 2 and 3 were performed with $T \ll T_c^d$, the bulk d -wave transition temperature. We now proceed to examine the temperature dependence. In Fig. 4 we have plotted the normalized temperature dependence of $|\Delta^{(p_x)}(0)|^2$ (circles) and $|\Delta^{(d)}(\infty)|^2$ (crosses), these being the p -wave *like* order parameter at the interface and the bulk d -wave order parameter respectively. As we can see $|\Delta^{(p_x)}(0)|^2$ is a linear function of temperature over a wide range (from $T \sim 0.1t$ to $0.4t$). Extrapolating this linear dependence we can state that $|\Delta^{(p_x)}(0)|^2$ would go to zero at a temperature of around

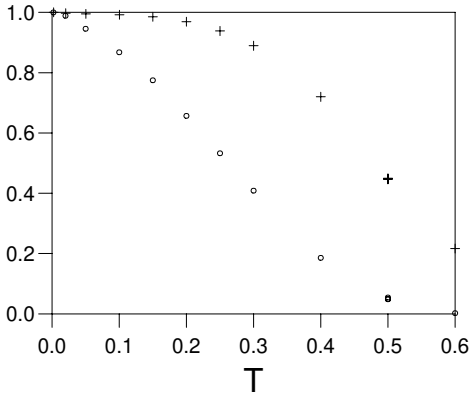


FIG. 4. The temperature dependence of the p -wave component of the order parameter, $\frac{|\Delta^{(p_x)}(0)|^2}{|\Delta^{(p_x)}(0)|_{T=0}^2}$ (circles), and the d -wave component, $\frac{|\Delta^{(d)}(\infty)|^2}{|\Delta^{(d)}(\infty)|_{T=0}^2}$ (crosses), T is measured in units of t .

$T_c^p \approx 0.5t$, if it were not coupled to the d -wave order parameter. From Fig. 4 we infer from the fact that $|\Delta^{(p_x)}(0)|^2$ deviates from a straight line above $T \approx 0.5t$ that it is enhanced above T_c^p by coupling to the d -wave order parameter.

This unusual temperature dependence of the p -wave like component can be explained by examining the phase diagram for a perfect square tight binding lattice. It is known that at half filling we have a ground state with a stable d -wave order parameter. However one can also define a separate T_c for extended s -wave or p -wave states. Near half filling T_c^d is greater than T_c^s or T_c^p and so only the d -wave state occurs in the bulk [24]. However if the d -wave and extended s -wave order parameters were suppressed somehow then the system would in principle go superconducting at T_c^p . Interestingly the T_c for the “ p -wave like” singlet order parameter $\Delta^{(p)}$ is the same as that of true triplet p -wave order parameter, which follows from the identical form of the gap equation in both cases [24]. In effect our phase slip has forced $\Delta^{(d)}$ and $\Delta^{(s)}$ to vanish at $x = 0$. This allows the intrinsic underlying p -wave state to become apparent. It would be interesting to test this underlying p -wave state experimentally, for example by tunneling experiments to see whether or not there is a finite gap inside a superconducting phase slip. If there is such a gap it would show that the pairing mechanism has attractive components for p -wave pairing as well as d -wave. This would only be true for some specific model pairing interactions, such as our nearest neighbour Hubbard model.

V. INTERFACE PROPERTIES: DEPENDENCE ON BARRIER.

Having considered the most simple case ($\epsilon_i = 0$ for all sites) we now focus our attention on what happens if we

have a finite tunnel barrier ($V \neq 0$) in region (I) of our system (Fig. 1). In this case it is also interesting to consider the situation where there is no phase slip over the interface and compare this to the result obtained when there is a phase slip. In this section we study three different strengths of barrier, where in region (I) we have defined $V/t = 1, 2, 5$.

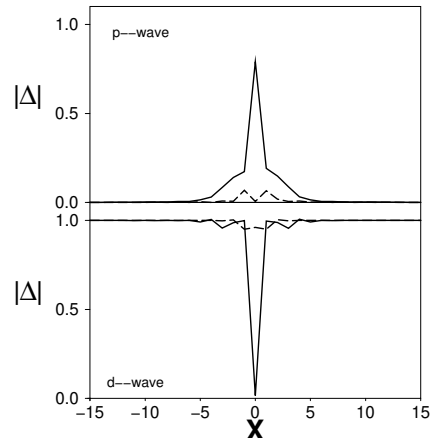


FIG. 5. Profiles of different symmetry components of the superconducting order parameter in the presence of no phase slip, $\theta = 0$, (solid lines), and a $\theta = \pi$ phase slip (dashed lines). The upper graph plots $|\Delta^{(p_x)}(x)|/|\Delta^{(d)}(\infty)|$ and the lower graph plots $|\Delta^{(d)}(x)|/|\Delta^{(d)}(\infty)|$. The barrier interface height is $V = t$ and temperature is $T = 0$.

In Fig. 5 we compare both $|\Delta^{(p_x)}(x)|$ and $|\Delta^{(d)}(x)|$ for the cases of (i) there is a phase slip across the interface (solid line) and (ii) when there is no phase slip (dashed line), for $V/t = 1$. From this figure we can see that as in the case of no barrier the phase slip means that $|\Delta^{(d)}(0)| = 0$. This then, effectively, induces a finite $|\Delta^{(p_x)}(0)|$ at the interface. However when there is no phase slip (dashed lines) we can see that although the $|\Delta^{(d)}(x)|$ is diminished in the region of the interface it does not go to zero, conversely now, due to the symmetry of the problem, $|\Delta^{(p_x)}(0)|$ must be zero. We have also calculated the extended s -wave component to the order parameter in the region of the interface. We find that the extended s -wave component is a maximum, at the interface, when there is no phase slip and zero when there is a phase slip, similar to Fig. 2.

Figs. 6 and 7 show the different components to the order parameter for larger strengths of barrier ($V/t = 2, 5$). What we see in these two figures is that as the barrier height is increased the differences between the $\theta = 0$ and $\theta = \pi$ cases becomes smaller. In the limit of a very high strength impurity barrier, Fig. 7, there is essentially no difference between the order parameter components whether a phase slip is present or not. Fig. 6, however, is more interesting. We see that when there is no phase slip $|\Delta^{(d)}(x)|$ is reduced in the region of the barrier, and as expected $|\Delta^{(p_x)}(0)|$ is zero. In the presence of a phase

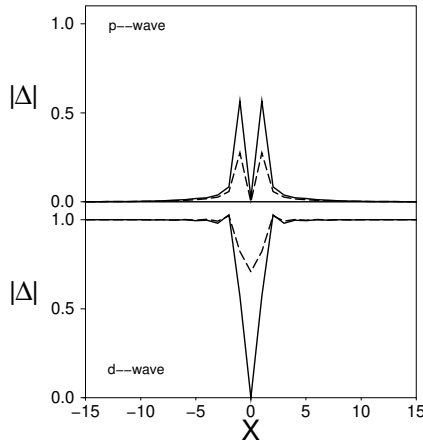


FIG. 6. Profiles of different symmetry components of the superconducting order parameter, for an intermediate barrier height, $V = 2t$. The plotted curves are otherwise exactly as in Fig. 5.

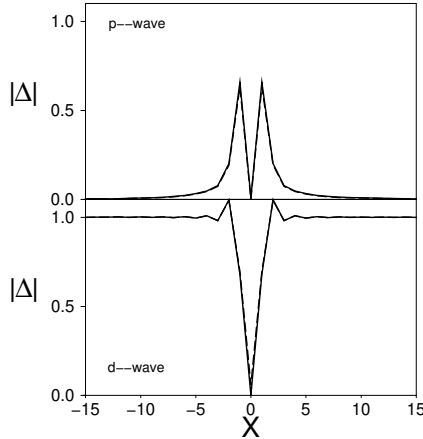


FIG. 7. Profiles of different symmetry components of the superconducting order parameter, for a large barrier height, $V = 5t$. The plotted curves are otherwise exactly as in Fig. 5.

slip, as in all the other cases, the $|\Delta^{(d)}(0)|$ is zero at the phase slip. But, unlike Figs. 2 and 5, $|\Delta^{(p_x)}(0)|$ is also zero. This shows that we have gone through three regimes at the interface. These being (i), low scattering at the interface where, $|\Delta^{(d)}(0)|$ is finite when there is no phase slip and $|\Delta^{(p_x)}(0)|$ is finite in the presence of a phase slip, (ii), intermediate scattering at the interface where, $|\Delta^{(d)}(0)|$ is still finite when there is no phase slip but now $|\Delta^{(p_x)}(0)|$ is zero in the presence of a phase slip and (iii), large scattering at the interface, $|\Delta^{(d)}(0)|$ is now zero when there is no phase slip and $|\Delta^{(p_x)}(0)|$ is also zero in the presence of a phase slip.

To see the physical origin of these three regimes we study the local particle density of states, $N(E)$, in the region of the interface. Figs. 8, 9, 10 and 11 show the density of states $N(E)$ for four strengths of barrier, $V/t = 0$,

1, 2 and 5, respectively. In these four figures we have plotted both the density of states in the presence of a phase slip, $N^\pi(E)$, (thick solid line) and in the absence of a phase slip, $N^0(E)$, (thin solid line). We also show the densities of states for four values of x , the distance from the interface.

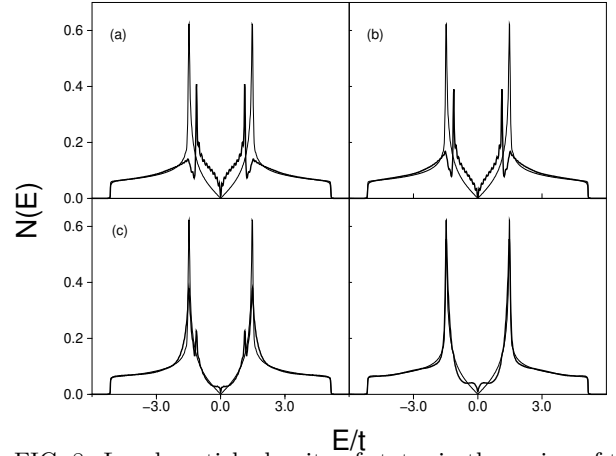


FIG. 8. Local particle density of states in the region of the interface when the barrier height is $V = 0$. We consider both a phase slip (thick solid line) and no phase slip (thin solid line). The curves plotted are (a) $x = 0$, (b) $x = 1$, (c) $x = 2$ and (d) $x = 3$.

In the first case we consider $V/t = 0$ (Fig. 8). The first thing to note is that the density of states in the absence of a phase slip corresponds to the pure bulk lattice d -wave density of states. This is simply because for $V = 0$ and $\theta = 0$ there is no interface. However the density of states in the presence of a phase slip, $N^\pi(E)$ does change in as we move away from the interface. Comparing $N^0(E)$ and $N^\pi(E)$ we see a dramatic shift in the density of states in the region of the Fermi energy. We can see in Fig. 8(a) that there is a strong shift of spectral weight from the peaks into the region near the Fermi level. We see that the gradient of the local particle density of states, in the region of $E = 0$ is dramatically changed, and the size of the gap, (the distance between the two peaks) is strongly reduced in the presence of a phase slip. Moving away from $x = 0$ (Figs 8(b), 8(c) and 8(d)) we see that these large changes in density of states gradually diminish with x until $N^0(E)$ and $N^\pi(E)$ become nearly identical. Interestingly the energy region near $E = 0$ is most strongly affected when x is large, corresponding to the long-range nature of the energy states associated with the d -wave gap node [35,36].

There is a very strong contrast between the case $V = 0$ in Fig. 8 and the case $V/t = 1$ shown in Fig. 9. In Fig. 9 we see that $N^0(E)$ (thin solid line) has no subgap structure at all, and this is quite different to the dramatic subgap structure obtained for $N^\pi(E)$.

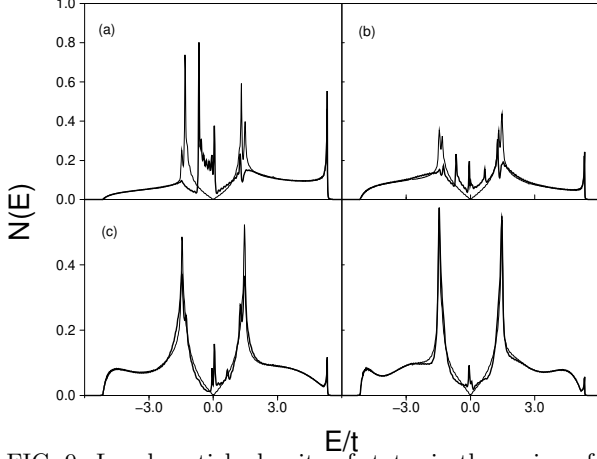


FIG. 9. Local particle density of states in the region of the interface when the barrier height is weak, $V = t$. The plotted curves are otherwise exactly as in Fig. 8.

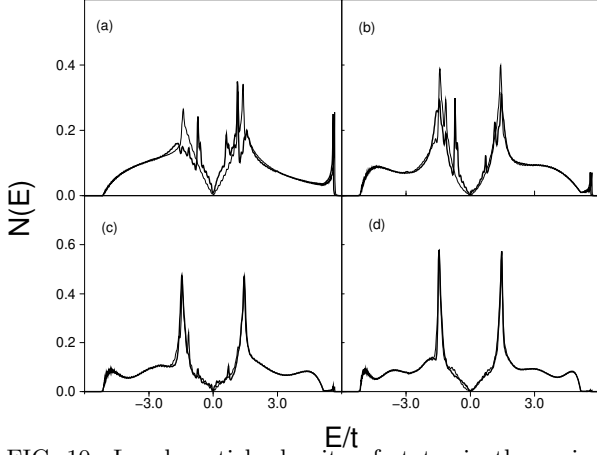


FIG. 10. Local particle density of states in the region of the interface when the barrier height is intermediate, $V = 2t$. We consider both a phase slip (thick solid line) and no phase slip (thin solid line). The curves plotted are (a) $x = 1$, (b) $x = 2$, (c) $x = 3$ and (d) $x = 4$.

As we increase the barrier strength to $V/t = 2$ (Fig. 10) we still see that there is no subgap structure in $N^0(E)$ whereas $N^\pi(E)$ still has some subgap structure, although this structure is not as dramatic as in Fig. 9. In Fig. 10 we have only plotted $N^0(E)$ and $N^\pi(E)$ for $x \neq 0$ because the $x = 0$ density of states is dominated by states well away from the gap region.

In Fig. 11 we see that in the presence of a very strong barrier, $V/t = 5$, $N^0(E) = N^\pi(E)$ suggesting that the two sides to the interface have become effectively decoupled. Also in this limit there is no resonant structure in either $N^0(E)$ or $N^\pi(E)$.

Finally we estimate the Josephson critical current as a function of the barrier height, by determining the Josephson energy. This is defined by

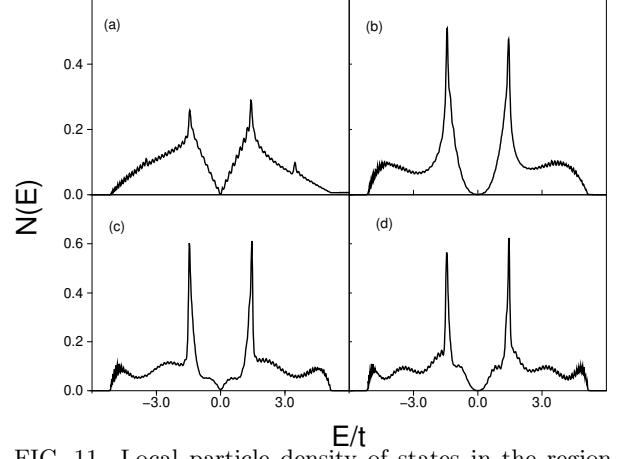


FIG. 11. Local particle density of states in the region of the interface when the barrier height is strong, $V = 5t$. The plotted curves are otherwise exactly as in Fig. 10.

$$E_J = \frac{1}{2} (E(\pi) - E(0)) \quad (10)$$

where we estimate the energy difference from the integrated densities of states

$$E(\phi) = \int_{-\infty}^0 N(\phi)(E) dE \quad (11)$$

for $\phi = \pi$ and $\phi = 0$ respectively. The critical current is approximately proportional to this energy difference,

$$I_c \propto E_J \quad (12)$$

where the constant of proportionality depends on the form of the $E(\phi)$ relationship. In the simple Josephson tunneling case $E(\phi) - E(0) = E_J \sin \phi$, and $I_c = E_J$, but in general other forms of $E(\phi)$ are possible. For example we have found that $E(\phi)$ is approximately sawtooth in grain boundary junctions [28] and there is experimental evidence for non-sine wave behaviour [37].

In Fig. 12 we have plotted the calculated critical current (I_c) as a function of the strength of the impurity potential (ϵ/t) in region I. In this figure we have normalized the critical current with respect to the critical current when no barrier is present. What we again observe is consistent with the three different regimes (i), little or no normal scattering at the interface, where there is no sub gap resonant structure but $N^\pi(E) \neq N^0(E)$ for $|E| < |\Delta^{(d)}|$, (ii), moderate normal scattering at the interface, where there is sub gap resonant structure in $N^\pi(E)$ but not in $N^0(E)$ and finally (iii), large normal scattering at the interface, where $N^\pi(E) \approx N^0(E)$. From this it is possible to deduce that, as one would expect for a high strength interface barriers, the Josephson Critical Current approaches zero. The three regimes are visible in the calculated I_c of Fig. 12: in the first weak decrease in I_c with barrier height, the intermediate regime where there is a strong decrease in I_c , and in the strong scattering regime where $I_c \rightarrow 0$.

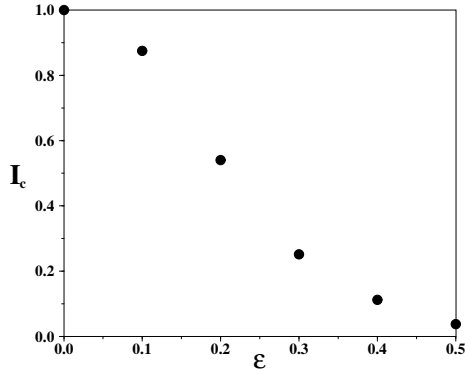


FIG. 12. The normalized Josephson critical current as a function of interface barrier height, V/t .

VI. CONCLUSIONS.

In this paper we have investigated the properties of a d -wave order parameter in the region of a (100) interface between two $d_{x^2-y^2}$ superconductors. We have determined how the barrier height at the interface influences the local density of states and Josephson current. In particular we could identify three distinct regimes with qualitatively different behaviour, corresponding to weak, intermediate and strong barriers, respectively.

We have also calculated the subdominant extended s -wave, and p -wave like order parameter components at the interface. In particular we have shown that the p -wave component has a temperature dependence which reveals the underlying bulk T_c for p -wave pairing, even though this is normally hidden by the higher bulk d -wave T_c . In principle a tunneling experiment could be carried out to test whether or not this p -wave component occurs in real systems. Such an experiment would provide qualitatively new information about the form of the microscopic pairing interaction.

VII. ACKNOWLEDGMENTS.

This work was supported by the EPSRC under grant number GR/L22454 and the TMR network Dynamics of Nanostructures. We would like to thank B.L Györfy, J.J. Hogan O'Neill and J.P. Wallington for useful discussions.

[1] D.J. Scalapino, Phys. Rep. **250**, 329 (1995).
[2] D.J. van Harlingen, Rev. Mod. Phys. **67**, 515 (1995).
[3] J.F. Annett, N. Goldenfeld, A.J. Leggett in Physical Properties of High Temperature Superconductors, Vol. 5, D.M. Ginsberg (ed.) (World Scientific, Singapore, 1996).
[4] K.A. Kouznetsov et al., Phys. Rev. Lett. **79**, 3050 (1997).

[5] A. Bhattacharya *et al.*, Phys. Rev. Lett. **82**, 3132 (1999).
[6] M. Matsumoto and H. Shiba, J. Phys. Soc. Jpn. **64**, 3384 (1995).
[7] M. Matsumoto and H. Shiba, J. Phys. Soc. Jpn. **64**, 4867 (1995).
[8] M. Matsumoto and H. Shiba, J. Phys. Soc. Jpn. **65**, 2194 (1996).
[9] A.M. Martin and J.F. Annett, Phys. Rev. B **57**, 8709 (1998).
[10] M. Covington *et al.*, Phys. Rev. Lett. **79**, 277 (1997).
[11] W. Belzig, C. Bruder and M. Sigrist, Phys. Rev. Lett. **80**, 4285 (1998).
[12] Y. Tanaka, Phys. Rev. Lett. **72**, 3871 (1994).
[13] Y.S. Barash, A.V. Galaktionov and A.D. Zaikin, Phys. Rev. B **52**, 665 (1995).
[14] J.X. Zhu, Z.D. Wang, and H.X. Tang, Phys. Rev. B **54**, 7354 (1996).
[15] H.X. Tang, Z.D. Wang and J.X. Zhu, Phys. Rev. B **54**, 12509 (1996).
[16] A. Huck, A. van Otterlo and M. Sigrist, Phys. Rev. B **56**, 14163 (1997).
[17] C.R. Hu, Phys. Rev. Lett. **72**, 1526 (1994).
[18] J.H. Xu, J.H. Miller and C.S. Ting, Phys. Rev. B **53**, 3604 (1996).
[19] Y.S. Barash, A.A. Svidzinsky and H. Burkhardt, Phys. Rev. B **55**, 15282 (1997).
[20] A.M. Martin and J.F. Annett, Superlattices and Microstructures, **25** 1019 (1999).
[21] Y. Tanuma, Y. Tanaka, M. Yamashiro and S. Kashiwaya, Physica C **282**, 1857 (1997).
[22] Y. Tanuma, Y. Tanaka, M. Yamashiro and S. Kashiwaya, Physica C **293**, 234 (1997).
[23] A. Gurevich and E.A. Pashitskii, Phys. Rev. B **57**, 13878 (1998).
[24] J. F. Annett and J.P. Wallington, In *Symmetry and Pairing in Superconductors*, eds. M Asuloos and S. Kruchinin, NATO ASI Proceedings. Dordrecht (Kluwer, 1998).
[25] R. Haydock, in: Solid state Physics, **35**, eds. Ehrenreich, F. Seitz and D. Turnbull (Academic Press, New York, 1980).
[26] J.F. Annett and N.D. Goldenfeld, J. Low Temp. Phys. **89**, 197 (1992).
[27] G. Litak, P. Miller and B.L. Györfy, Physica C **251**, 263 (1995).
[28] J.J. Hogan-O'Neill, A.M. Martin and J.F. Annett, Phys. Rev. B **60**, 3568 (1999).
[29] C.N. Yang, Phys. Rev. Lett. **63**, 2144 (1989).
[30] B.L. Györfy, J. Staunton and M. Stocks, Phys. Rev. B **44**, 5190 (1991).
[31] J.F. Annett, Adv. Phys. **39**, 83 (1990).
[32] O. Entin-Wohlman and J. Bar-Sagi, Phys. Rev. B **18**, 3174 (1977).
[33] Y. Tanaka and M. Tsukada, Phys. Rev. B **42**, 2066 (1990).
[34] F. Sols and J. Ferrer, Phys. Rev. B **49**, 15913 (1994).
[35] A.V. Balatsky, M.I. Salkola, Phys. Rev. Lett. **76**, 2386 (1996).
[36] I. Kosztin and A.J. Leggett, Phys. Rev. Lett. **79**, 135 (1997).
[37] E. Il'ichev *et al.*, Phys. Rev. Lett. **81**, 894 (1998).